ELSEVIER

Coordination Chemistry Reviews 225 (2002) 201–214

COORDINATION CHEMISTRY REVIEWS

www.elsevier.com/locate/ccr

Structural and functional models of nitrile hydratase

Pradip K. Mascharak *

Department of Chemistry and Biochemistry, University of California, Santa Cruz, CA 95064, USA

Received 28 March 2001; accepted 19 June 2001

Contents

Abstract

Nitrile hydratase, the enzyme involved in microbial nitrile assimilation, comprises either one non-heme low-spin iron(III) or a non-corrinoid cobalt(III) center at the active site. Two carboxamido nitrogens, one cysteine-sulfur, and two sulfurs from a cysteine-sulfenic (Cys-SO) and a cysteine-sulfinic (Cys-SO_2) acid moiety respectively constitute the donor set around the metal center of this hydrolytic enzyme. Binding of one molecule of NO at the sixth site of the iron(III) center modulates the activity of the enzyme. It is suggested that a metal-bound hydroxide could be involved in the hydration of nitriles. Attack of water (or hydroxide) on a metal-bound nitrile is another possibility. During the past few years, modeling work by several groups have provided a great deal of insight into the structure and function of nitrile hydratase. Structural and spectroscopic studies on iron(III) and cobalt(III) complexes of various designed S,N-containing ligands have shown that the unusual coordination structure of the M(III) site (a) raises its potential and shuts off any redox activity, (b) allows binding of NO at the sixth site and oxidative modification of the bound S donors, and (c) brings the pK_a of metal-bound water close to 7. Attempts to synthesize catalytically active model complexes have met with limited success. This review includes the results and implications of the modeling studies reported so far.

Keywords: Nitrile hydratase; Structural and functional models; Hydration studies

1. Introduction

The enzyme nitrile hydratase (NHase) is a key player in the process of assimilation of nitriles by microorganisms via hydration to amides [1–9]. Interest in this

* Tel.: +1-831-459-4251; fax: +1-831-459-2935.
E-mail address: pradip@chemistry.ucsc.edu (P.K. Mascharak).

0010-8545/02/$ - see front matter
PII: S0010-8545(01)00413-1

enzyme has grown since its successful application in industrial production of amides. During the past ten years, a considerable amount of research effort has been directed toward studying smaller model complexes that mimic the active site(s) of NHase. The goal of such pursuit is to establish the role of the non-heme iron(III) (or non-corrinoid cobalt(III)) center of NHase in the process of hydration of organic nitriles (RCN) in the biosphere. It is also expected that selected model complexes could serve as synthetic catalysts in the production of amides. This review highlights the results of the investigations with model complexes reported so far. Brief discussions on nitriles in the environment and the enzyme have been included as the background of the review.

2. Background

2.1. Organic nitriles in the environment

Nitrile-containing compounds (RCN) are essential components in the metabolic cycle of higher plants and many soil microorganisms [1,2]. In plants, they have a widespread occurrence across several phyla where they serve as: (1) growth hormones during plant germination, (2) natural products of plant metabolites, and (3) constituents of a chemical defense system that guard plants from herbivores [10–12]. 3-Indoleacetonitrile and its derivatives (structure (i)) are abundant in plants. These compounds play a fundamental role in plant growth during the process of germination and in plant phototropism. Another family of organic nitriles in plants is the cyanoglycosides (structure (ii)) [12]. These nitriles release cyanide under mild conditions. The plants use them as chemical protective agents against casual herbivores.

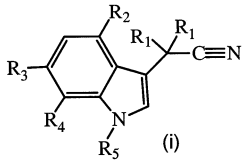

(i)

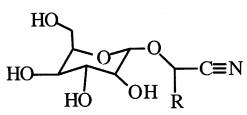

(ii)

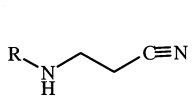

(iii)

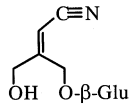

(iv)

To date, over 2000 species of plants have been identified to be cyanogenic by having cyanoglycosides in their roots, seeds or leaves. Plants also contain cyanoalkaloids, cyanolipids (structure (iii)), and other small molecular weight nitrile-containing natural products (an example is structure (iv)) that have other hitherto unknown functions [13,14]. Most plants release organic nitriles as a major portion of their root exudates [15]. This process has resulted in the evolution of microorganisms that assimilate nitriles from the rhizosphere and use them as their only source of carbon and nitrogen [2]. Most of these microorganisms utilize hydrolytic enzymes to hydrolyze the nitrile group of the plants exudates and obtain the corresponding carboxylic acid and ammonia products which they use as metabolites to make the essential elements of their biomass (DNA, RNA, and protein constituents). Microbes that assimilate organic nitriles from the environment belong to two Eubacterial phyla: the Purple bacteria and Gram-positive bacteria. It is interesting to note that these phyla share a common evolutionary origin as it was determined by a phylogeny study based on sequence comparisons of 16 S rRNA. This suggested that microorganisms that assimilate nitriles from the environment may have evolved from a common ancestor several million years ago and also advocates for a primeval presence of nitriles in the early environment of earth.

Organic nitriles are also produced in megaton scales for the manufacture of plastics, fibers, pesticides, reagents for water treatment, and other fine chemicals. Several nitriles of anthropogenic origin are, however, toxic and exhibit carcinogenic and teratogenic properties [16,17]. Acrylonitrile [18–20] and pesticides like bromoxynil [21,22] are now considered as threats to the environment. The industries also generate enormous quantities of nitrile-containing chemical wastes that are often difficult to dispose of. Most of the time, the nitriles are present in dilute aqueous solutions which cannot be incinerated. Presently, industrial wastes with toxic nitriles are either disposed at sea or pumped into deep pressure wells below the water table [23].

2.2. Enzymes involved in nitrile assimilation

Microbial enzymes that catalyze the hydrolysis of organic nitriles are divided into two main classes: the nitrilases and the nitrile hydratases. The nitrilases hydrolyze organic nitriles in one step to the corresponding carboxylic acid and ammonia products and they do not use metal cofactors for catalysis. On the other hand, the nitrile hydratases hydrolyze organic nitriles to the corresponding amide product [4–9]. Participation of other enzymes such as amidases completes the hydrolysis of the terminal amide to the corresponding acid and ammonia products (Scheme 1). Hereafter, the review will focus on NHase and more specifically on the models of NHases.

NHases contain either a non-heme iron(III) center or a non-corrinoid cobalt(III) center at their active site depending on the organisms and are subdivided into two classes: (1) the iron-containing NHases (Fe–NHases) [24–33]; and (2) the cobalt-containing NHases

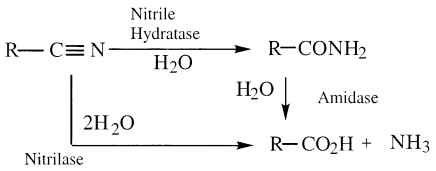

Scheme 1.

(Co–NHases) [34–36]. The enzyme generally consists of α and β subunits and exists as αβ 46 kDa heterodimers or $(\alpha\beta)_2$ 92 kDa tetramers. Several groups have reported that NHase functions as an αβ heterodimer (with one metal center) and that its fragmentation into individual subunits inactivates the enzyme. Since NHases exhibit significant protein sequence homology, especially at their metal binding domain in the α subunit where a highly conserved -C-S-L-C-S-C- motif is noted, it is believed that all NHases possibly have the same structure and similar mechanism of catalysis. The relatively more robust Co–NHases have wider substrate specificity. In recent years, NHases from several organisms (and related mutants) have been employed as biocatalysts in industrial production of acrylamide in kiloton quantities [3–7,37,38] and in enantioselective syntheses of other fine chemicals with amide groups [39–45]. NHases have also been used in environmental remediation of nitriles [46–49].

2.3. Properties and structures of Fe–NHases

The Fe–NHases are readily characterized by their grayish green colors. They exhibit an electronic absorption spectrum with bands in the visible region at 700 and 420 nm, which arise from the iron center in these enzymes (Fig. 1). These enzymes also exhibit a rhombic electron paramagnetic resonance (EPR) spectrum with *g*-values at 2.28, 2.14, 1.97 which is characteristic of a low-spin ($S = 1/2$) iron(III) center (Fig. 1) [50]. Unlike other non-heme iron centers in biology [51,52] the iron(III) center of the NHase does not participate in redox reaction(s) and acts as a Lewis acid. The activity of one subset of the Fe–NHases, namely *Rhodococcus* N-774 [30], N-771 [31], and *Brevibacterium* R-312 [27] is photoregulated in vivo by nitric oxide (NO) via a reaction that involves reversible binding of NO at the Fe(III) site. Binding of NO in dark results in deactivation of the enzyme, a process that is reversed by loss of NO upon illumination [3,53–56]. This phenomenon is not observed with Co–NHases. The Fe–NHases are also inactivated by N_3^-, CN^-, and by metal ions like Hg^{2+} and Ag^+ [29].

The first structure of a NHase was determined by Nelson and coworkers in 1997 [57]. This group reported the structure of the Fe–NHase from *Brevibacterium* R312 (tetrameric $\alpha_2\beta_2$) at 2.66 Å resolution. The α subunit of this NHase consists of a long N-terminal arm and a rich α-helix region and it ends with an unprecedented fold at the C-terminal domain. The β subunit also contains a long N-terminal extension and it interacts strongly with the α subunit. A large subunit interface area of 3800 $Å^2$ and the tight contact suggest that a strong interaction between the two subunits is essential for the function of the enzyme. In a second crystallographic study, Endo and coworkers have determined the structure of the NO-inactivated Fe–NHase from *Rhodococcus* sp. N-771 at 1.7 Å resolution [58]. Since the two NHases are homologous by the sequence, the two structures are very similar. However, the latter structure is more precise and hence it offers additional structural information regarding the metal binding domain of NHase that was not revealed in the structure reported by Nelson and coworkers.

In both structures, the iron(III) center is located in a cleft situated at the interface of the two subunits of the αβ heterodimer. The coordination structure of this active site is quite unusual. The low resolution structure shows that the iron(III) center is ligated to two *deprotonated* carboxamido nitrogens from the αCys113-αSer114 peptide backbone and three sulfur thiolates from the αCys110, αCys113, and αCys115 amino acid residues [57]. The high resolution structure by Endo and coworkers [58] further reveals that two of the

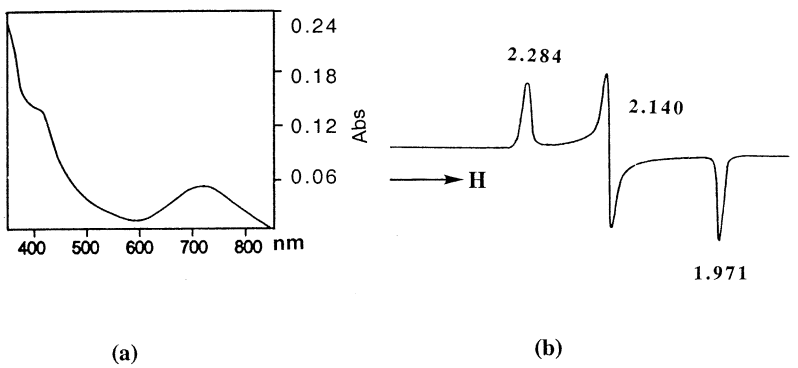

Fig. 1. (a) Electronic absorption spectrum and (b) EPR spectrum of Fe–NHase from *Brevibacterium* R312.

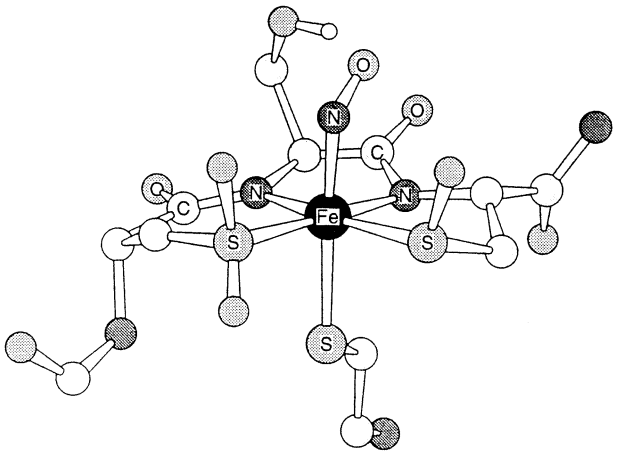

Fig. 2. Structure of the NO-bound iron site of *Rhodococcus* sp. N-771 NHase.

cysteine sulfurs bound on the basal plane of the iron(III) center are post-translationally modified to the sulfinic (αCys112-SO_2) and sulfenic (αCys114-SO) groups [59] and that a molecule of NO is coordinated at the solvent exposed site of the metal center (Fig. 2). The modified cysteine residues have also been observed in the mass spectra of the tryptic digest of purified NO-inactivated Fe–NHase [60].

The donor set of the iron(III) site of the Fe–NHases namely, carboxamido N and sulfe(i)nato RSO_x ($x = 1$, 2) groups is unprecedented. Coordination of deprotonated carboxamido N has only been discovered recently in the nitrogenase P cluster [61] while ligation of modified cysteine (αCys-SO_x) residues to metal is yet to be discovered in a metalloenzyme. The effect(s) of the modified Cys-S centers on the overall properties of the iron(III) site is therefore an open question in the chemistry of the NHase at this time. In addition, Endo and coworkers have recently shown that reconstituted NHase, assembled from recombinant unmodified α and β subunits under argon, exhibit no NHase activity [62]. However, the protein is readily activated upon exposure to atmospheric oxygen. It thus appears that post-translational modification of the Cys-residues is essential for the catalytic activity.

The presence of a coordinated NO molecule at the apical site of the iron(III) center of the inactive NO-bound *Rhodococcus* sp. N-771 Fe–NHase [58] explains the mode of inactivation of Fe–NHases by NO. The active form of Fe–NHase, however, does not contain NO and raises question regarding the nature of the sixth ligand at the iron site of the active enzyme. Although the low-resolution structure of the active enzyme, reported by Nelson and coworkers [57], failed to identify the nature of the sixth ligand at the axial site of the iron(III) center, various spectroscopic studies have provided clues regarding this ligand. Results of early X-ray absorption study on the active form of Fe–NHase from *Brevibacterium* sp. R312, indicate the presence of a six-coordinate FeS_3E_3 (E = N and or O) chromophore at the active site [63]. Broadening of the EPR signals of the Fe–NHase from *Brevibacterium* sp. R312 upon addition of $H_2^{17}O$ suggests the presence of an exchangeable water molecule at the apical site of the iron(III) center of NHase [50]. More recently, pulsed electron nuclear double resonance (ENDOR) data have indicated that the ligand bound to the iron(III) center in NHase could be hydroxide (OH^-) [64].

2.4. Properties and structures of Co–NHases

The Co–NHases belong to a small group of cobalt-dependant enzymes in nature [65]. They are also the first examples of enzymes that incorporate a non-corrinoid cobalt(III) center in their structure(s). Although there is no report on the structure of a Co–NHase so far, results of X-ray absorption studies [66] and identical sequence homology at the metal binding region between the two types of enzymes (Fe– and Co–NHase) strongly suggest that the structure of the active site of Co–NHase is very similar to that of the Fe–NHase.

2.5. Mechanism(s) of nitrile hydration by NHases

The mechanism of catalysis by NHases remains unresolved at this time. Nelson and coworkers have suggested three plausible mechanisms of catalysis which are shown in Fig. 3 [57]. In the first postulated mechanism (Fig. 3a), the nitrile substrate displaces a hydroxide ligand from the coordination sphere of the M(III) center and the metal-bound nitrile undergoes hydrolysis by a water molecule. The reaction generates a metal-

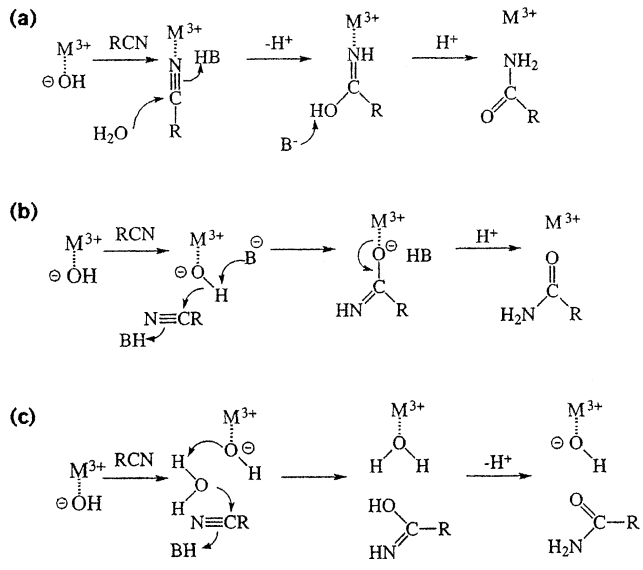

Fig. 3. Possible mechanisms of nitrile hydration by NHase [57].

bound imminol intermediate that rearranges to the amide product and then the amide is released. This is known as the inner-sphere mechanism. The presence of a molecule of iodoacetonitrile in close proximity of the iron(III) center noted in crystallographic work by Nelson and coworkers provides some support to this mechanism. There is also precedence for platinum(II) and rhodium(II) complexes that bind nitriles and catalyze their hydrolysis via an inner-sphere mechanism [67,68].

The second postulated mechanism (Fig. 3b), known as the outer-sphere mechanism, involves a nucleophilic attack of the metal-bound hydroxide on the nitrile substrate nested at the active site pocket. The reaction generates a transient imminolate species that is O-bonded to the metal. This species then rearranges to amide and is released as product. In the third postulated mechanism (Fig. 3c), the metal-bound hydroxide causes deprotonation of a free water molecule near the active site. It is the newly generated hydroxide that carries out the hydrolysis of the nitrile substrate. The eventual rearrangement of the hydrolyzed intermediate leads to the amide product. This mechanism is known as the second outer-sphere mechanism of catalysis. Note that in this mechanism, no substitution occurs at the coordination sphere of the M(III) center.

Since the coordination structures of the M(III) sites of the Fe– and Co–NHase are assumed to be very similar or identical, one expects that the two M(III) sites function in very similar ways. Support for this argument comes from the kinetic data available for these enzymes. The Co–NHase from *Rhodococcus rhodochrous* sp. J1 and Fe–NHase from *Brevibacterium* R312 hydrolyze propionitrile at almost identical rates under the same reaction conditions (1600 and 1800 mmol min^{-1}, respectively). When one considers the distinctly different kinetic labilities of low-spin iron(III) (d^5) and cobalt(III) (d^6) centers, a similar reactivity of the two NHases suggests that an outer-sphere mechanism of catalysis (i.e. one involving no ligand exchange) is most possibly in operation. However, there is no evidence that supports this hypothesis so far.

3. Model complexes and their reactivities

3.1. Required features and synthetic difficulties

The desire to understand the unusual hydrolytic chemistry of the iron(III) and cobalt(III) sites of the NHases has prompted efforts to synthesize smaller model complexes that reproduce both the structure and function of the active sites of Fe– and Co–NHases. Such efforts, often dubbed as 'synthetic analogue approach' have provided great insights into the intrinsic properties of the active sites of metallobiomolecules [69] and to date, research on analogues of the Fe– and Co–NHases has similarly afforded valuable information on the function of the metalloenzyme. The following sections highlight the results of the model studies reported so far.

In principle, good structural and functional models of NHase should include the following structural and functional features.

1. The mononuclear iron(III) or cobalt(III) center is ligated to carboxamido N and thiolato S donor centers with one or more of the thiolato S in the sulfenato and/or sulfinato form.
2. The reduction potential of the iron(III) site is high and hence it does not exhibit redox behavior and just functions as a Lewis acid.
3. The metal center has an open or solvent-bound coordination site. When this site is occupied by water, one expects that the pK_a of the bound water is close to 7. Whether nitriles bind to this site or not remains to be established.
4. The iron(III) center exhibits reactivity toward NO. Binding of NO converts the low-spin iron(III) site to a diamagnetic iron(III)–NO adduct. Upon illumination, the iron center loses NO readily.

If indeed one could synthesize such iron(III) and/or cobalt(III) model complex(es), then it is reasonable to expect that studies on the hydrolysis of nitriles with such species will provide important clues relating to the mechanism of the hydrolysis by the NHases.

In general, monomeric iron(III) complexes that comprise thiolato S and carboxamido N donor centers are quite scarce [70]. Most reactions with ferric ions and thiolates either afford S-bridged polymers or undergo auto-redox reactions that generate thiyl radicals ($RS^{\bullet}$) and iron(II) species. These reactions impede the isolation of the iron(III) species [71–73]. Moreover, coordination of carboxamido N to iron(III) centers was believed to be 'improbable' for a long time [74]. Since the pH necessary for deprotonation of the carboxamido N is too high for iron(II) and iron(III) to exist in aqueous solution (both ions precipitate as hydroxides at $pH \geq 3$) [75], it had generally been concluded that ligation of the deprotonated peptide N to iron was improbable. This paradigm discouraged many research groups from synthesizing such complexes. The situation has, however, been changed in recent years following isolation of several iron complexes with coordinated carboxamido nitrogens [70]. Overall, the scarcity of good models of NHase stems from the inherent difficulties one encounters in the synthesis of iron(III) (and cobalt(III)) complexes with carboxamido N and thiolato S donors. As described below, the majority of the NHase models have so far been synthesized with S-containing Schiff-base ligands.

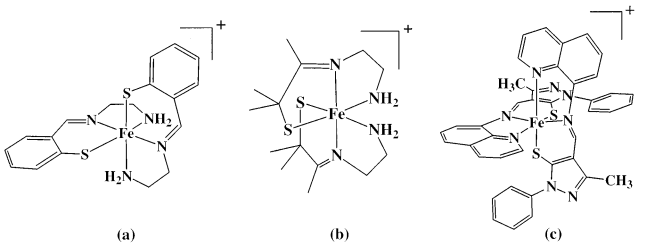

Fig. 4. Structures of: (a) $[Fe^{III}(S–sal:N^{\bullet}(CH_2)_2{}^{\bullet}NH_2)_2]^+$ (cation of **1**); (b) $[Fe^{III}(ADIT)_2]^+$ (cation of **2**); and (c) $[Fe^{III}(L^{N_2S})_2]^+$ (cation of **3**).

3.2. Models of Fe–NHases: complexes with thiolato S and amine/imine N donors

In 1975, Gatehouse and coworkers reported the first iron(III) complex with a mixed N, S coordination sphere although it was not reported as a NHase model [76]. The complex, bis-[*N*-(2-aminoethyl)thiosalicylideneiminato]iron(III) chloride, $[Fe^{III}(S–sal:N(CH_2)_2NH_2)_2]Cl$ (**1**), was synthesized via a metal-initiated template reaction in which ethylenediamine and 2-mercaptobenzaldehyde were added to iron(III) chloride in methanol. Complex **1** consists of a six-coordinate iron(III) center in a distorted octahedral geometry with two ligated 2-aminoethylsalicylidene-iminato tridentate units (Fig. 4a) [76]. The average length of the Fe–S bonds in this complex, 2.21 Å, is significantly shorter than the sum of the appropriate covalent radii (Fe, 1.34 and S, 1.04 Å). This suggests that a significant interaction exists between the p and d orbitals of sulfur and the d orbitals of iron. Both the magnetic moment (2.00 μ_B) and the rhombic EPR signal with *g*-values of 2.16, 2.12, 2.00 are consistent with a low-spin ($S = 1/2$) electronic configuration of the iron(III) center in **1** [77].

Kovacs and coworkers synthesized a similar iron(III) complex in 1995 and introduced it as a model for the low-spin non-heme iron(III) site in Fe–NHase [78]. This group followed the same in situ condensation on a metal template developed by Gatehouse. However, they used α-mercaptoacetone with ethylenediamine and iron(III) chloride in basic methanol and isolated bis(6-amino-2,3-dimethyl-4-azahex-3-ene-2-thiolato)iron(III) chloride, $[Fe^{III}(ADIT)_2]Cl$, (**2**). The iron(III) center in $[Fe^{III}(ADIT)_2]^+$ contains two thiolato sulfurs, two immino nitrogens, and two amine (NH_2) nitrogens in the first coordination sphere (Fig. 4b). The average Fe–S bond distance in **2** is 2.20 Å and is significantly shorter than that reported for Fe–NHase (2.32 Å) [57,58]. This difference could be due to the small bite of the ligand. Complex **2** comprises an iron(III) center which is low-spin ($S = 1/2$) at all temperatures as indicated by its magnetic moment (1.85 μ_B) and its EPR spectrum in methanol glass ($g = 2.19$, 2.13, 2.01). The electronic absorption spectrum of this complex in acetonitrile (two bands with maxima, λ_{max}, at 718 and 438 nm) resembles the absorption spectrum of the Fe–NHase in aqueous buffer.

Nivorozhkin and coworkers have reported a mononuclear iron(III) complex with the tridentate ligand [*N*,*N*′-bis(5-mercapto-3-methyl-1-phenylpyrazol-4-ylmethylene)ethylenediamine] as a spectroscopic model for the iron(III) site in Fe–NHase [79]. The structure of this complex, namely $[Fe^{III}(L^{N_2S})_2](ClO_4)$ (**3**) reveals that the iron(III) center has a distorted octahedral geometry with two thiolato sulfurs, two imine nitrogens, and two quinoline ring nitrogens as donors (Fig. 4c). The average Fe–S bond distance in **3** (2.28 Å) compares well with those reported for the other iron(III) complexes described above. Complex **3** is also low-spin ($S = 1/2$) and exhibits a magnetic moment of 1.95 μ_B. In chloroform glass (77 K), it displays a rhombic EPR signal with *g*-values 2.19, 2.13, and 1.98. The electronic absorption spectrum of this blue–green complex in chloroform consists of two bands with λ_{max} at 995 and 750 nm.

Mascharak and coworkers have studied the chemistry of the iron(III) complexes of two Schiff-base ligands namely, *N*-2-mercaptophenyl-2′-pyridylmethylenimine (PyASH) and *N*-2-mercapto-2-methylpropyl-2′-pyridylmethylenimine (PyMSH) [80]. The iron(III) complexes $[Fe^{III}(PyAS)_2](BPh_4)$ (**4**) and $[Fe^{III}(PyMS)_2](BPh_4)$ (**5**) have been synthesized by oxidizing the corresponding iron(II) complexes by ferrocenium salts [81]. In **4** and **5**, the deprotonated ligands are coordinated in *mer* fashion with two thiolato sulfurs *cis* to each other (Fig. 5). Both complexes are low-spin and exhibit rhombic EPR spectra (Fig. 6).

It is important to note at this point that six-coordinate iron(III) Schiff-base complexes with N_xO_y donor sets like $[Fe(N_2O)_2]^+$, $[Fe(N_3O_2)L]^+$ and $[Fe(N_4O_2)]^+$ are either high-spin ($S = 5/2$) or exhibit spin equilibria [82,83]. Even the hexadentate Schiff-base ligands with N_4O_2 donor set do not afford low-spin ($S = 1/2$) iron(III) complexes [84]. Thus the O-analogue of tridentate Schiff-base ligands like AMITH, ADITH and PyASH (Fig. 7) give rise to iron(III) complexes of the type $[Fe(N_2O)_2]^+$ which are either high-spin or exhibit spin equilibria.. In contrast, Schiff-base ligands with N_2S donor set like ADITH, AMITH, PyASH and PyMSH all afford iron(III) bis complexes that are

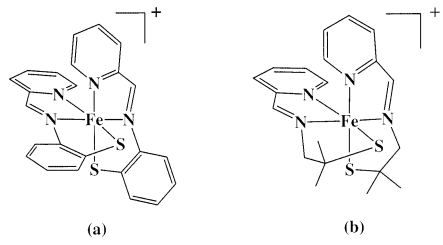

Fig. 5. Structures of: (a) $[Fe^{III}(PyAS)_2]^+$ (cation of **4**) and (b) $[Fe^{III}(PyMS)_2]^+$ (cation of **5**).

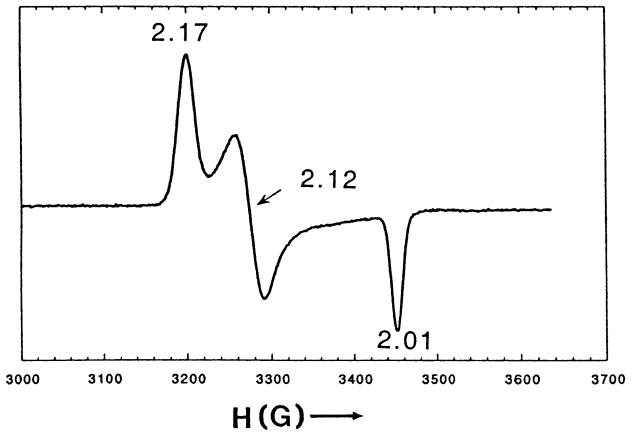

Fig. 6. X-band EPR spectrum of $[Fe^{III}(PyAS)_2]^+$ in DMF glass at 8 K.

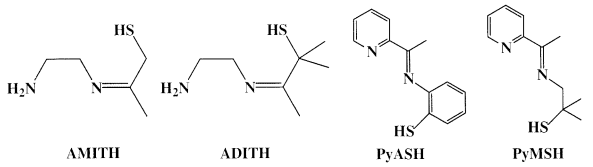

Fig. 7. Schiff-base ligands used for nitrile hydratase models.

low-spin at all temperatures. The change in spin configuration due to replacement of O with S in these ligands clearly indicates stronger interaction between thiolato sulfur and iron(III) center. Most of these species also exhibit thiolate-to-iron(III) charge transfer bands in the 550–850 nm range.

The first NHase model that comprises three thiolato sulfurs in a six-coordinate environment has been reported by Wieghardt and coworkers [85]. This iron(III) complex is derived from the hexadentate ligand 1,4,7-tris(4-*tert*-butyl-2-mercaptobenzyl)-1,4,7-triazacyclononane which provides three thiolato sulfurs and three amine-type nitrogens as the donor set. To avoid the auto-redox process known to take place between iron(III) salts and organic thiolates, this group either reacted the ligand with $[Fe^{III}(acac)_3]$ or with $[Fe^{II}(OAc)_2]$ in methanol and exposed the reaction mixture to air 'carefully' to produce the desired complex (1,4,7-tris(4-*tert*-butyl-2-mercaptobenzyl)-1,4,7-triazacyclononane)iron(III), $[Fe^{III}(L^{N_3S_3})]$ (**6**). The structure of this complex revealed a six-coordinate pseudo-octahedral iron(III) center with three amine nitrogens from the triazacyclononane ring and three thiolato S atoms coordinated in a *fac*-fashion around the metal center (Fig. 8). In $[Fe^{III}(L^{N_3S_3})]$, the average Fe–S distance is 2.28 Å and compares well with the corresponding distance reported for the other complexes that have only two thiolato S donors. Interestingly, the average $Fe–N_{amine}$ distance in **6** is 2.08 Å and is very close to the $Fe–N_{amido}$ distance noted for NHase (2.07 Å). However, its spectroscopic parameters are very different from those reported for NHase. For example, **6** exhibits a solution magnetic moment of 2.4 μ_B at 77 K which rises to 3.7 μ_B at 300 K. Also, the EPR spectrum of solid **6** at 10 K displays an isotropic signal with $g = 4.3$ corresponding to a typical high-spin Fe(III) ($S = 5/2$) species. The electronic absorption spectrum of **6** in acetonitrile consists of two bands in the visible region with λ_{max} at 775 and 651 nm. It is interesting to note that although **6** contains three thiolato sulfur donors in the coordination sphere, the iron(III) center remains high-spin. Wieghardt and coworkers have also reported the synthesis and properties of the corresponding iron(III) complex with alkylthiolato groups connected to the triazacyclononane frame. This Fe(III) complex is also high-spin at all temperatures and displays one electronic absorption band at 551 nm.

Recently, in a series of papers, Kovacs and coworkers have reported the synthesis and reactivity of a coordinatively unsaturated iron(III) complex that comprises two thiolato sulfurs, two imine-type nitrogens, and one amine-type nitrogen in the coordination sphere. This group synthesized the iron(III) complex 2,3,13,14-tetramethyl-4,8,12-triaza-3,12-pentadeca-diene-2,14-dithiolato iron(III) via ferrocenium oxidation of the corresponding iron(II) species prepared by in situ condensation of 3-methyl-3-mercapto-2-butanone and 3,3′-iminobis(propylamine) in presence of Fe(II) chloride [86]. The structure of the pentacoordinate iron(III) complex, namely $[Fe^{III}S_2^{Me_2}N_3(Pr,Pr)]PF_6$ (**7**), consists of an iron(III) center in a distorted trigonal bipyramidal geometry in which the thiolates are positioned in the basal plane and the two imine nitrogens are at the axial positions (Fig. 9a). The average Fe–S distance noted for

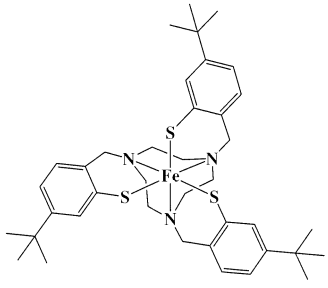

Fig. 8. Structure of $[Fe^{III}(L^{N_3S_3})]$ (**6**).

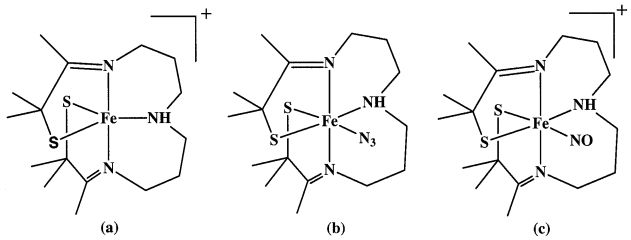

Fig. 9. Structures of: (a) $[Fe^{III}S_2^{Me_2}N_3(Pr,Pr)]^+$ (cation of **7**); (b) $[Fe^{III}S_2^{Me_2}N_3(Pr,Pr)(N_3)]$; and (c) $[Fe^{III}S_2^{Me_2}N_3(Pr,Pr)(NO)]^+$.

7 (2.14 Å) is significantly shorter than the corresponding distance in the other complexes and in NHase. It is quite possible that the absence of the carboxamido nitrogens (negatively charged) in the coordination sphere allows the ligated thiolates to interact more strongly with the iron(III) center of the complex and gives rise to short Fe(III)–S_{thio} distances. This complex is high-spin at room temperature as evident from its magnetic moment of 5.0 μ_B at 300 K. However, the magnetic moment drops to 2.0 μ_B below 50 K and the low temperature EPR spectrum in methanol glass ($<$ 150 K) displays a rhombic signal ($g = 2.20$, 2.15, 2.00). These results indicate that the low-spin state is significantly populated at low temperatures. The electronic absorption spectrum of $[Fe^{III}S_2^{Me_2}N_3(Pr,Pr)]^+$ in methanol consists of one band with λ_{max} at 416 nm which is quite different from the electronic spectrum of Fe–NHase (λ_{max} at 700 and 420 nm). However, when $[Fe^{III}S_2^{Me_2}N_3(Pr,Pr)]^+$ binds azide (N_3^-) in acetonitrile to form the corresponding azide adduct namely $[Fe^{III}S_2^{Me_2}N_3(Pr,Pr)(N_3)]$ (Fig. 9b), the electronic absorption spectrum becomes very similar to that of the Fe–NHase. Thus, $[Fe^{III}S_2^{Me_2}N_3(Pr,Pr)(N_3)]$ has absorbances with λ_{max} at 708 and 460 nm. Also, the azide adduct is low-spin and exhibits a rhombic EPR signal in methanol glass ($g = 2.23$, 2.16, 1.99). These spectral features make the azide adduct a good model of the azide-inhibited form of the Fe–NHase. The relatively open S–Fe–N angle (132.3(2)°) in the basal plane of **7** (Fig. 9a) allows binding of azide to the iron(III) center of **7** and in $[Fe^{III}S_2^{Me_2}N_3(Pr,Pr)(N_3)]$, azide is *trans* to a thiolato sulfur (Fig. 9b). Binding of azide is reversible and the extent of binding depends both on the temperature and the nature of the solvent. Interestingly, **7** does not bind nitriles under any conditions.

The five-coordinate complex $[Fe^{III}S_2^{Me_2}N_3(Pr,Pr)]^+$ deserves further attention due to its ability to bind one molecule of NO to generate the corresponding diamagnetic ($S = 0$) nitrosyl adduct $[Fe^{III}S_2^{Me_2}N_3(Pr,Pr)(NO)]^+$ [87]. Structural characterization of this species reveals that the iron(III) center has a distorted octahedral geometry in which NO is coordinated *trans* to a thiolato sulfur (Fig. 9c). The X-ray absorption spectrum of this NO-adduct resembles that of the dark-adapted (NO-bound) Fe–NHase from *Rhodococcus* sp. R312 [88]. Also, the NO-adduct $[Fe^{III}S_2^{Me_2}N_3(Pr,Pr)(NO)]^+$ displays the IR stretch corresponding to the nitrosyl group (ν_{NO}) at 1822 cm^{-1} close to the ν_{NO} of NO-inactivated enzyme (1853 cm^{-1}) [54,55]. The Fe–N–O moiety in $[Fe^{III}S_2^{Me_2}N_3(Pr,Pr)(NO)]^+$ is, however, quite linear (172.3°). It thus appears that there is greater backbonding in the Fe–NO unit of this model complex compared to that in the Fe–NO moiety in the NO-inactivated Fe–NHase where the Fe–N–O angle is 158.6°. This difference could arise from the absence of sulfenic (R*S*O) and/or sulfinic groups (R*S*O_2) at the coordination sphere of the model complex. Interestingly, exposure of $[Fe^{III}S_2^{Me_2}N_3(Pr,Pr)(NO)]^+$ to a strong UV-light source (Hg lamp) for 6 h results in the loss of NO from the complex [87]. However, the researchers also observed that the metal complex undergoes irreversible decomposition.

3.3. Models of Fe–NHases: complexes with thiolato S and carboxamido N donors

The model complexes described above do not include carboxamido nitrogens and/or sulfe(i)nato (R*S*O/R*S*O_2) moieties in the coordination sphere of the iron(III) centers. Since these are some essential features of the metal site in NHases, several groups have undertaken the task of isolation and characterization of iron(III) complexes of designed ligands with varying number of thiolato sulfur and carboxamido nitrogen donor centers. Studies on such complexes have provided valuable insight into the role(s) of such coordination in the overall reactivity of the iron(III) centers in NHases. A major portion of work in this area has been completed by Mascharak and coworkers during the period 1997–2001.

The first model complex with thiolato sulfurs and carboxamido nitrogens was reported by Mascharak and coworkers in 1998. Reaction of $(Et_4N)[FeCl_4]$ with deprotonated designed ligand $PyPepS^{2-}$ (where $PyPepSH_2$ = *N* - 2 - mercaptophenyl - 2′ - pyridinecarboxamide, Hs denote the dissociable peptide and thiol H) in DMF affords $(Et_4N)[Fe^{III}(PyPepS)_2]$ (**8**) in good yield. The geometry around the iron(III) center in **8** is octahedral with the two essentially planar tridentate ligand frames coordinated in *mer* fashion (Fig. 10a) [89]. Complex **8** exhibits an Fe(III)–N_{amido} distance of 1.954(2) Å which is very similar to that observed in other iron(III) complexes with coordinated carboxamido nitrogens [70,90–93]. Coordination of carboxamido nitrogens to iron(III) in **8** is readily indicated by the shift of ν_{CO} to 1612 from 1666 cm^{-1} in free $PyPepSH_2$ [70]. The iron(III) center of this model complex is low-spin in the temperature range 8–300 K and its EPR spectrum ($g = 2.22$, 2.14, 1.98) resembles that of the enzyme very closely. In

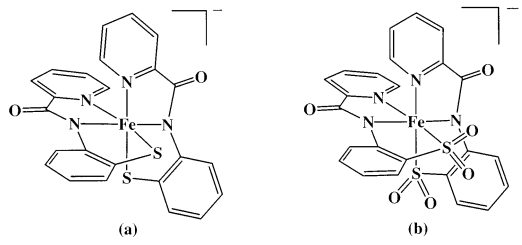

Fig. 10. Structures of: (a) $[Fe^{III}(PyPepS)_2]^-$ (anion of **8**) and (b) $[Fe^{III}(PyPepSO_2)_2]^-$ (anion of **9**).

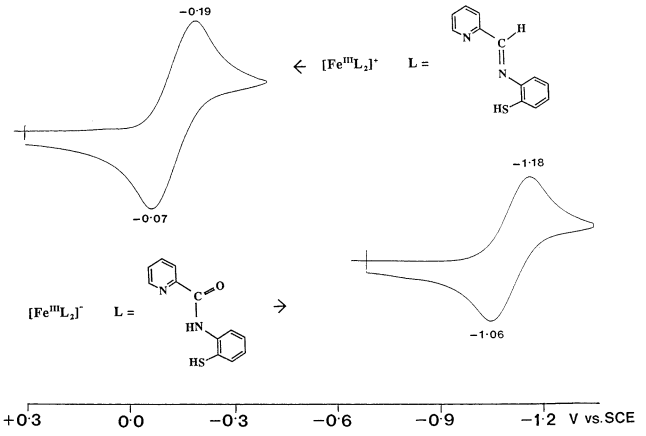

Fig. 11. Cyclic voltammograms of $(Et_4N)[Fe^{III}(PyPepS)_2]$ (**8**) and $[Fe^{III}(PyAS)_2](BPh_4)$ (**4**) in DMF (0.1 M $(Et_4N)(ClO_4)$, Pt electrode, 50 mV s^{-1} scan rate). Potentials are shown vs. aqueous saturated calomel electrode.

addition, **8** exhibits a thiolate-to-iron(III) charge transfer band at 850 nm in water.

The synthesis of the model complex **8** affords some interesting clues regarding ligation of carboxamido nitrogens to iron. First, no reduction of iron(III) takes place upon mixing of $PyPepS^{2-}$ with iron(III) salts. Under similar conditions, addition of $PyAS^-$ (Fig. 7) to iron(III) salts causes immediate reduction of iron and only the iron(II) complex is obtained from the reaction mixture. It thus appears that ligands like $PyPepSH_2$ that employ carboxamido nitrogens in addition to thiolato sulfurs to bind iron prefer iron(III) centers. Indeed, $PyPepSH_2$ does not react with iron(II) salts at all. Second important point to note is the stability of **8** in aqueous medium. Although the complex is synthesized in DMF, it is quite stable in protic solvents and does not afford oxo- or hydroxo-bridged dimeric or polymeric iron(III) species which are often recognized as thermodynamically very stable entities in the hydrolytic chemistry of iron [75]. Finally, formation of **8** as the only product in the reaction mixture indicates that thiolate-bridged multinuclear iron complexes are not very common when the ligands contain additional carboxamide groups [70].

The electrochemical properties of **8** provides the most important clue regarding the role of carboxamido nitrogens in the redox behavior of the iron(III) center in Fe–NHase. In DMF, $(Et_4N)[Fe^{III}(PyPepS)_2]$ (**8**) and $[Fe^{III}(PyAS)_2](BPh_4)$ (**4**) exhibit their half-wave potentials ($E_{1/2}$) at -1.12 and -0.13 V (vs. SCE, saturated calomel electrode), respectively (Fig. 11). This dramatic shift of 1 V in $E_{1/2}$ clearly indicates that the coordination of negatively charged strong-field carboxamido nitrogens provide significant stability to the $+3$ oxidation state of iron in non-heme iron species [70,89,94]. The presence of carboxamido nitrogens and thiolato sulfurs around the iron(III) site in NHase thus raises the redox potential of the iron site. The high reduction potential in turn does not allow the iron(III) site of NHase to participate in any redox process; rather it acts as a Lewis acid in the process of hydration of nitriles.

When H_2O_2 is added to a cold solution of **8** in DMF, a deep green solution (λ_{max} 690 nm) results from which $Na[Fe^{III}(PyPepSO_2)_2]$ (**9**) has been isolated [95]. Crystallographic studies on $[Fe^{III}(PyPepSO_2)_2]^-$ reveal that the process of oxidation affords the corresponding sulfinato complex (Fig. 10b). This model complex from Mascharak's group is the first example of a iron(III) species with both carboxamido nitrogen and S-bonded sulfinato groups around the metal center. The S–O distance in **9** (average 1.472(4) Å) compares well with the same observed with other known sulfinato species and the coordinated sulfinato groups display ν_{SO} at 1184 cm^{-1}. Complex **9** is low-spin and it dissolves in water, acetonitrile, and DMF to produce green solutions. The aqueous solution is indefinitely stable and exhibits an electronic absorption spectrum (λ_{max} at 700 and 420 nm) almost identical to that of the Fe–NHase. This work demonstrates for the first time, that oxidation of iron(III) complexes with coordination sphere resembling that of the active site of Fe–NHase can be oxidized to give sulfinato species. Interestingly, attempts to oxidize $[Fe^{III}(PyAS)_2](BPh_4)$ (**4**) under similar conditions only result in decomposition of the iron complex.

Very recently, Mascharak and coworkers have synthesized the iron(III) complex of the designed pentadentate ligand $PyPSH_4$ (Fig. 12) [96]. Despite coordinative unsaturation, the model complex $(Et_4N)[Fe^{III}(PyPS)]$ (**10**) remains mononuclear. In **10**, the iron(III) center is coordinated to two carboxamido nitrogens, two thiolato sulfurs and one pyridine ring nitrogen (Fig. 12). The average $Fe–N_{amido}$ and $Fe–S_{thio}$ distances are 2.038(2) and 2.312(2) Å, respectively. This blue–green model complex is particularly notable since it allows one to examine for the first time, the reactivity of the iron(III) center toward various molecules including nitriles. The iron(III) center in **10** binds to a variety of ligands (methanol, PhO^-, PhS^-, py, *N*-Me-imidazole) at low temperature and gives rise to green solutions with a band around 700 nm. Such bindings are re-

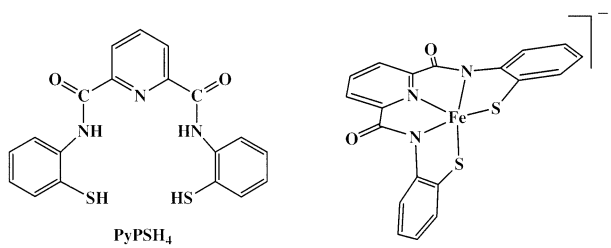

Fig. 12. Structures of $PyPSH_4$ and $[Fe^{III}(PyPS)]^-$ (anion of **10**).

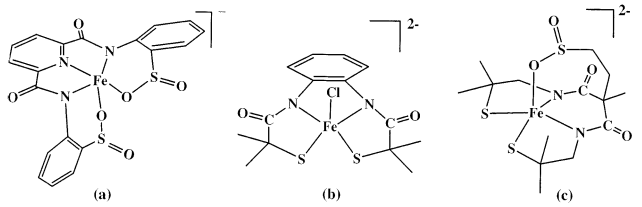

Fig. 13. Structures of: (a) $[Fe^{III}(PyP\{SO_2\}_2)]^-$ (anion of **11**); (b) $[Fe^{III}(N_2S_2)Cl]^{2-}$ (anion of **12**); and (c) $[Fe^{III}(L^{N_2S_3O_2})]^{2-}$ (anion of **13**).

versible and the six-coordinate $[Fe^{III}(PyPS)L]^{n-}$ species are all low-spin with g-values very close to those of the Fe–NHase. These results indicate that the iron(III) site of the functional enzyme is six-coordinate. The pK_a of the water bound at the iron(III) site of **10** has been determined (at -30 °C) to be 6.3 ± 0.4. It is important to note that **10** (like **7**) does *not* show any affinity toward nitriles. It thus appears that at physiological pH, a metal-bound hydroxide promotes hydration of nitriles nested at the active site pocket of Fe–NHase (mechanism 3b or 3c).

Limited exposure of a solution of **10** (in acetone) to dioxygen results in the formation of a bis-sulfinic species. This reaction mimics the post-translational modification of the Cys-S center in Fe–NHase. The structure of the more stable O-bonded sulfinato complex $(Et_4N)[Fe^{III}(PyP\{SO_2\}_2)]$ (**11**, Fig. 13a) has been determined [96]. It appears that oxidation of coordinatively unsaturated $[Fe^{III}(PyPS)]^-$ (**10**) gives rise to the O-bonded sulfinato complex **11** while coordinatively saturated species $[Fe^{III}(PyPepS)_2]^-$ (**8**) affords the S-bonded sulfinato complex **9**. This is further supported by the fact that six-coordinated low-spin cyanide adducts of the S-bonded and O-bonded sulfinato complexes namely, $Na_2[Fe^{III}(PyP\{SO_2\}_2)(CN)]$ and $(Et_4N)_2[Fe^{III}(PyP\{SO_2\}_2)(CN)]$ have been isolated by starting from six- and five-coordinate species, respectively. These low-spin cyanide adducts afford green solutions in water and other solvents. The $E_{1/2}$ values of $(Et_4N)[Fe^{III}(PyPS)]$ and $(Et_4N)[Fe^{III}(PyP\{SO_2\}_2)]$ in DMF (-0.65 and -0.36 V vs. SCE) indicate that the iron(III) centers in these two model complexes are quite stabilized much like the iron(III) site in Fe–NHase ($E_{1/2}$ in aqueous buffer $= -0.48$ V vs. SCE [97]). Comparison of the structure, properties, and reactivity of $(Et_4N)[Fe^{III}(PyPS)]$ (**10**) with those of the iron(III) site of Fe–NHase suggests that **10** is indeed a very good model of the active site of the Fe–NHase.

Two additional iron(III) complexes with ligands containing carboxamido nitrogen and thiolato sulfur donors have recently been reported. The first one has been reported by Artaud et al. in a short review on nitrile hydratase [97]. These researchers have employed the previously known ligand *N*,*N*′-1,2-phenylenebis-(2-mercapto-2-methylpropionamide), developed by Hans and Krüger who synthesized its copper complex [98]. The structure of the iron(III) species, namely, $(Et_4N)[Fe^{III}(N_2S_2)Cl]$ (**12**) reveals that the iron(III) center exists in a square pyramidal geometry in which two carboxamido nitrogens and two thiolato sulfurs are bonded in the basal plane while a chloride ion is coordinated at the axial position (Fig. 13b). In $[Fe^{III}(N_2S_2)Cl]^-$, the average Fe–N_{amido} distance is 1.92 Å which is somewhat shorter than the corresponding distance in NHase (2.07 Å). Also, the average Fe–S_{thio} distance in **12** (2.19 Å) is shorter than the corresponding distance in NHase. Despite the fact that the iron(III) center in $[Fe^{III}(N_2S_2)Cl]^-$ has structural features similar to the active site of Fe–NHase, its physical parameters are very different from those reported for the enzyme. For example, **12** displays a broad EPR spectrum in DMF at 10 K with g-values of 5 and 3.5 which is indicative of an intermediate spin state ($S = 3/2$) for the iron(III) center. Also, the electronic absorption spectrum of **12** in CH_2Cl_2 consists of only one band in the visible region with λ_{max} at 500 nm. The red color of this model complex is distinctly different from that of the green enzyme (λ_{max} at 700 and 420 nm).

In a recent communication, Chottard and coworkers have reported the synthesis and structure of the second iron(III) complex that comprises two carboxamido nitrogens, two thiolato sulfurs and one O-bonded sulfinato SO_2 donor in its coordination sphere [99]. The iron(III) center in this model complex is ligated to 2-methyl-2-thiomethylmalonylenebis-(2-mercapto-2-methylpropionamide) forming $(Et_4N)_2[Fe^{III}(L^{N_2S_3O_2})]$ (**13**), a square pyramidal complex with two carboxamido nitrogens and two thiolato sulfurs in the basal plane (Fig. 13c). The axial position is occupied by one oxygen atom of the sulfinato group. In $[Fe^{III}(L^{N_2S_3O_2})]^{2-}$, the average Fe–$N_{amido}$ and Fe–S_{thio} distances are 1.95 and 2.22 Å, respectively. The Fe–SO_2 bond distance in **13** (2.00 Å) compares well with the corresponding distance in **11** (1.91 Å). Accidental exposure to air most possibly gives rise to the sulfinato group in **13** although the researchers have so far been unable to isolate the tris-thiolato species. It is important to note that here again, one obtains the O-bonded sulfinato isomer of the coordinatively unsaturated iron(III) precursor much like the oxidation of **10** leading to **11**.

Although $(Et_4N)_2[Fe^{III}(L^{N_2S_3O_2})]$ (**13**) is a good structural model for the active site of Fe–NHase, its spectroscopic properties are surprisingly very different from those of the enzyme. Indeed, the spectroscopic parameters of **13** are more similar to those of **12**. For example, **13** exhibits an intermediate spin state ($S = 3/2$) as is evident from its solid state magnetic moment of 3.8 μ_B at all temperatures (3–300 K). This was also supported by its broad EPR spectrum with g-values centered at

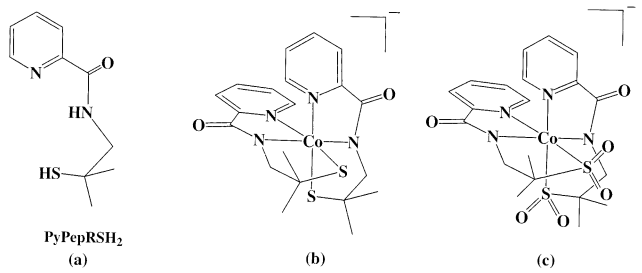

Fig. 14. Structures of: (a) $PyPepRSH_2$; (b) $[Co^{III}(PyPepRS)_2]^-$ (anion of **15**); and (c) $[Co^{III}(PyPepRSO_2)_2]^-$ (anion of **17**).

3.75 and 2.01 (DMF glass at 10 K). Furthermore, the electronic absorption spectrum of **13** in MeCN consists of only one band with λ_{max} at 475 nm. Collectively, these results suggest that proper disposition of the carboxamido nitrogens and the thiolato sulfurs (including the modified ones) around the iron(III) center is crucial in determining the overall spectroscopic (and electronic) parameters of the metal center in the model complexes. As revealed in the X-ray studies (Fig. 2), the iron(III) center of a good model complex should be coordinated to a thiolato sulfur at the axial position while the carboxamido nitrogens and the modified sulfe(i)nato groups should be ligated in the basal plane.

3.4. Models of Co–NHases: complexes with thiolato S and carboxamido N donors

Modeling work in this area began with the assumption that the coordination structures of the active sites of the Fe–NHase and the Co–NHase are very similar or identical. Mascharak and coworkers reported the first set of cobalt(III) complexes of ligands containing both carboxamido nitrogen and thiolato sulfur donors. The cobalt(III) complex of the designed ligand $PyPepSH_2$ namely, $(Me_4N)[Co^{III}(PyPepS)_2]$ (**14**) is structurally very similar to the corresponding iron(III) complex **8** (see Fig. 10a) [95]. This octahedral diamagnetic cobalt(III) complex has two thiolato sulfurs in *cis* positions while the two carboxamido nitrogens are *trans* to each other. In **14**, the avarage Co(III)–N_{amido} and Co(III)–S_{thio} bond distances are 1.917(3) and 2.222(3) Å, respectively. A similar cobalt(III) complex with a ligand with alkyl thiolates $PyPepRSH_2$ (Fig. 14a) has also been reported by this group [100]. The presence of *gem*-dimethyl group next to the thiolate donor allows isolation of the monomeric bis complex $Na[Co^{III}(PyPepRS)_2]$ (**15**, Fig. 14b) in which the coordination structure around the cobalt(III) center is similar to that in **14**. Both these complexes have been synthesized via reaction of $[Co(NH_3)_5Cl]Cl_2$ with the deprotonated ligands in DMF at 60 °C. The unusual use of a kinetically inert cobalt(III) starting material in these syntheses is noteworthy.

Reaction of H_2O_2 with solutions of **14** or **15** in methanol at 0 °C readily affords the corresponding sulfinato complexes $Na[Co^{III}(PyPepSO_2)_2]$ (**16**) and $Na[Co^{III}(PyPepRSO_2)_2]$ (**17**, Fig. 14c) in high yield [100]. Similar oxidation is also observed when methanolic solutions of **14** and **15** are exposed to oxygen. These reactions are comparatively slow. However, the process of oxidation can be accelerated by the addition of activated charcoal to the reaction mixtures. The clean conversion of the thiolato sulfurs to the S-bonded sulfinato groups can be followed by absorption spectroscopy and mass spectrometry. The reddish brown color of the solutions of **14** and **15** arises from a strong thiolate-to-cobalt(III) charge transfer transition around 500 nm. This band disappears upon oxidation of the thiolato sulfurs to sulfinic groups.

A functional model of Co–NHase has recently been reported by Mascharak and coworkers who utilized the designed ligand $PyPSH_4$ (Fig. 12) in synthesizing a mononuclear cobalt(III) species with hydroxide as one of the ligand [101]. Reaction of $PyPS^{4-}$ with $[Co(NH_3)_5Cl]Cl_2$ in DMF results in the formation of the dimeric complex $(Et_4N)_2[Co^{III}_2(PyPS)_2]$ (**16**) in which each cobalt(III) center attains six coordination by forming one thiolato bridge (Fig. 15a). Further reaction of **16** with $(Et_4N)(CN)$ in acetonitrile affords the monomeric cyanide-adduct $(Et_4N)_2[Co^{III}(PyPS)(CN)]$ (**17**) in which the cobalt(III) center is bonded to two carboxamido nitrogens (*trans* to each other), two thiolato sulfurs (*cis* to each other), one pyridine nitrogen, and a cyanide (Fig. 15b). This model complex resembles the proposed cyanide-inhibited cobalt(III) site of Co–NHase in terms of the coordination structure. The Co–C and C–N distances of the Co–CN unit (1.896(12) and 1.149(13) Å, respectively) of **17** compare well with those in other cobalt(III) complexes with cyanide ligands. Both **16** and **17** are diamagnetic and the latter complex displays its ν_{CN} at 2111 cm^{-1}.

Complex **17** is stable when dissolved in acetonitrile or DMF. However, when it is dissolved in water (pH 7), CN^- is immediately lost and $[Co^{III}(PyPS)(H_2O)]^-$ is formed (reaction b, Scheme 2). This facile replacement of CN^- by water indicates that the enzyme-like coordination structure of the cobalt(III) center of **17** is *not* substitutionally inert. Clearly, the conventional wisdom of kinetic inertness of low-spin cobalt(III) centers is not

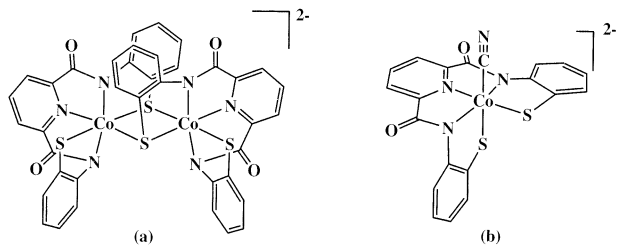

Fig. 15. Structures of: (a) $[Co^{III}_2(PyPS)_2]^{2-}$ (anion of **16**) and (b) $[Co^{III}(PyPS)(CN)]^{2-}$ (anion of **17**).

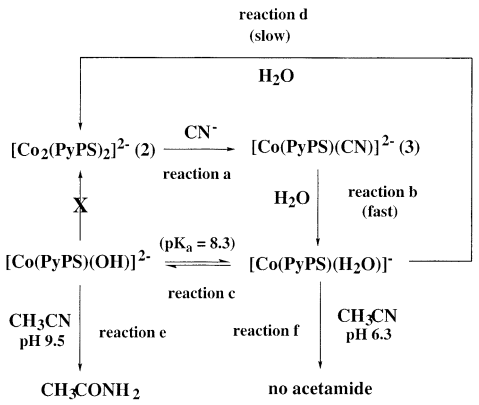

Scheme 2.

applicable to all cobalt(III) species and exceptions are found in complexes with specific donor centers (vide infra). The pK_a of the bound water in $[Co^{III}(PyPS)(H_2O)]^-$ has also been measured by Mascharak and coworkers [101]. Comparison of this pK_a value (8.3) with that of cobalt(III) complex $[Co^{III}(L)(H_2O)]^+$ (L = very similar pentacoordinate peptide ligands but with all nitrogen donors, p$K_a = 7$) [102] indicates that the thiolato sulfurs in $[Co^{III}(PyPS)(H_2O)]^-$ raise the pK_a of the bound water. The reactivity of $[Co^{III}(PyPS)(OH)]^{2-}$, the species present in pH 9 buffer is very noteworthy. As shown in Scheme 2, this species promotes rapid hydration of acetonitrile to acetamide at room temperature with multiple turnovers. Since the $[Co^{III}(L)(H_2O)]^+$ complex does not show such activity at pH 9, it is evident that the presence of thiolato sulfurs around the cobalt(III) center is crucial in promoting hydration of nitriles.

To date, $[Co^{III}(PyPS)(H_2O)]^-$ (obtained from **17**) is the only functional model of NHase that catalyzes hydration of nitriles at pH ≥ 8. Reaction e in Scheme 2 suggests that the enzyme-mediated hydration of nitriles could proceed via intermolecular attack of cobalt-bound hydroxide on nitriles nested in the active site pocket (mechanism b or c, Fig. 3). Since $[Co^{III}(PyPS)(H_2O)]^-$ does not initiate hydration at pH 6, the alternative mechanism in which nitriles first coordinate to cobalt(III) by replacing water and then get hydrolyzed (mechanism a, Fig. 3) is not supported.

Artaud and coworkers have reported the cobalt(III) complex of the ligand *N*,*N*′-1,2-phenylenebis-(2-mercapto-2-methylpropionamide) namely, $(Et_4N)[Co^{III}(N_2S_2)Cl]$ (**18**) [103]. This distorted square planar complex with short Co–N and Co–S bonds (1.882 and 2.134 Å, respectively) and triplet ($S = 1$) ground state does not interact with nitriles, H_2O, imidazole or OH^-. However, it binds two CN^- or two NO molecules. The IR spectrum of the dinitrosyl product exhibits two ν_{NO} at 1765 and 1820 cm^{-1}. The reactivity of **18** with NO is interesting although Co–NHases are not known to bind NO.

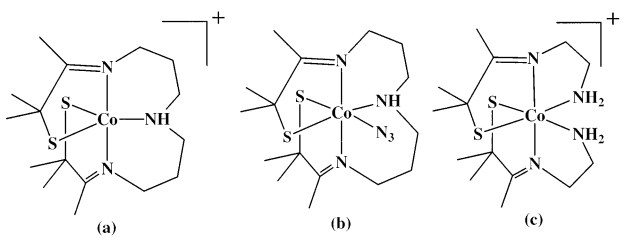

Fig. 16. Structures of: (a) $[Co^{III}S_2^{Me_2}N_3(Pr,Pr)]^+$ (cation of **19**); (b) $[Co^{III}S_2^{Me_2}N_3(Pr,Pr)(N_3)]$; and (c) $[Co^{III}(ADIT)_2]^+$ (cation of **20**).

3.5. Models of Co–NHases: complexes with thiolato S and amine/imine N donors

Kovacs and coworkers have employed their in situ condensation technique to synthesize the cobalt(III) analogue of **7** namely $[Co^{III}S_2^{Me_2}N_3(Pr,Pr)]PF_6$ (**19**) [104]. This five-coordinate trigonal bipyramidal cobalt(III) complex (Fig. 16a) is structurally very similar to **7** with Co–S_{thio} distance of 2.16(2) Å, which is shorter than that noted for most cobalt(III) thiolates. Complex **19** is intermediate spin ($S = 1$) and is reversibly reduced at $E_{1/2} = -0.46$ V versus SCE. The cobalt(III) center in **19** binds azide and SCN^- quantitatively at room temperature *trans* to one of the thiolates but exhibits no affinity toward NO, nitriles, and butyrate. The structure of the dark pink azide-adduct $[Co^{III}S_2^{Me_2}N_3(Pr,Pr)(N_3)]$ has been determined (Fig. 16b) [105]. As expected, the spectroscopic and structural parameters of $[Co^{III}S_2^{Me_2}N_3(Pr,Pr)(N_3)]$ resemble those of the six-coordinate cobalt(III) model complex $[Co^{III}(ADIT)_2](PF_6)$, (**20**, Fig. 16c) which has also been synthesized by this group via oxidation of the cobalt(II) species with ferrocenium salts [105]. Kinetic studies on azide- and thiocyanate binding by **19** reveals that the rate of temperature-dependent reversible binding of these ligands to the cobalt(III) center of **19** is of the order of 10^{-1} to 10^{-2} s^{-1}. Since these rates are comparable to those observed for the corresponding iron(III) complexes, it appears that the unique coordination environment at the active site of NHases gives rise to lability to both iron(III) and cobalt(III) centers despite low-spin configuration. This in turn provides an answer to why a kinetically inert low-spin cobalt(III) ion could be present at the active site of NHase and promote catalytic hydration of nitriles at significant speed [105].

Prolonged exposure to air converts **19** into the square pyramidal sulfinato/thiolato complex $[Co^{III}(S^{Me_2}(S^{O_2})N_3(Pr,Pr)]PF_6$ (**21**) in which only one of the thiolato sulfur is oxidized (Fig. 17a). Complex **21** is low-spin and exhibits S–O distance (1.453(2) Å) comparable to that noted for **17**. Interestingly, **21** does not bind azide or SCN^- to its open site, presumably due to strong *trans*-effect of the sulfinate group [104]. Addition of H_2O_2 to **21** results in the oxidation of the remaining thiolate to a sulfenate and the oxygen atom of the sulfenato group occupies the sixth site on cobalt in

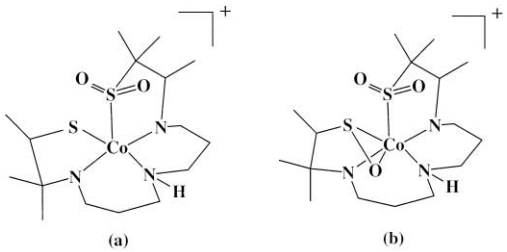

Fig. 17. Structures of: (a) $[Co^{III}(S^{Me_2}(S^{O_2})N_3(Pr,Pr)]^+$ (cation of **21**) and (b) $[Co^{III}(\eta^2\text{-}SO)(S^{O_2})N_3(Pr,Pr)]^+$ (cation of **22**).

$[Co^{III}(\eta^2\text{-}SO)(S^{O_2})N_3(Pr,Pr)]PF_6$ (**22**, Fig. 17b). No further oxidation of this sulfur center is observed, even upon prolonged treatment with H_2O_2. Complex **22** is the first example of a NHase model with sulfenato coordination. The S–O distance in **22** (1.548(3) Å) falls in the usual range. Unfortunately, lack of reactivity of both **21** and **22** prevents one from exploring the changes in reactivity of the cobalt(III) center upon incremental oxidation of the coordinated sulfur atoms.

4. Conclusions

To date, results of the modeling work ha'ye provided valuable insight into the unusual properties of the non-heme iron(III) site in NHase. For example, it is quite evident that coordination of carboxamido nitrogens to the iron(III) center of NHase raises its reduction potential and hence this iron site does not participate in any redox reaction in conjunction with dioxygen. It has also become clear that iron(III) and cobalt(III) centers with coordination structures similar to that in NHase are kinetically active and exhibit similar binding properties. In addition, the pK_a of water bound to such M(III) center is around 7. The model studies have also suggested that iron(III) centers with N, S coordination could bind NO although it is yet to be shown that such iron(III) nitrosyls are photolabile. Hydration studies with models like $[Co^{III}(PyPS)(H_2O)]^-$ (obtained from **17**) indicate that a metal-bound hydroxide could be responsible for the hydration of nitriles at the active site. It is expected that future studies with more robust and active model complexes will afford additional clues related to the unusual non-heme iron(III) (and non-corrinoid cobalt(III)) site in NHase.

Acknowledgements

Research in Mascharak's lab was supported by grants from the National Institute of General Medical Sciences and the National Science Foundation. P.M. thanks Dr Juan Noveron and Dana Marlin for help in preparing this manuscript.

References

[1] B. Vennesland, E.E. Conn, C.J. Knowles, J. Westley, F. Wissing, Cyanide in Biology, Academic Press, London, 1981.
[2] E.E. Conn, Cyanide Compounds in Biology, Wiley, Chichester, UK, 1988.
[3] I. Endo, M. Odaka, M. Yohda, Trends Biotechnol. 17 (1999) 244.
[4] M. Kobayashi, S. Shimizu, Nature Biotechnol. 16 (1998) 733.
[5] H. Yamada, M. Kobayashi, Biosci. Biotechnol. Biochem. 60 (1996) 1391.
[6] M. Kobayashi, T. Nagasawa, H. Yamada, Trends Biotechnol. 10 (1992) 402.
[7] T. Nagasawa, H. Yamada, Trends Biotechnol. 7 (1989) 153.
[8] C.M. Hjort, S.E. Godtfredsen, C. Emborg, J. Chem. Technol. Biotechnol. 48 (1990) 217.
[9] T. Nagasawa, H. Yamada, Trends Biotechnol. 7 (1989) 153.
[10] N. Takahashi, Chemistry of Plant Hormones, CRC Press, Boca Raton, FL, 1986.
[11] E.E. Conn, in: E.A. Ebell, B.V. Charlwood (Eds.), Secondary Plant Products. In: Encyclopedia of Plant Physiology, vol. 8, Springer, Berlin, 1980, pp. 461–492.
[12] R.D. Gibbs, Chemotaxonomy of Flowering Plants, McGill-Queens University Press, Montreal, 1974.
[13] F.F. Fleming, Nat. Prod. Rep. 16 (1999) 597.
[14] A.D. Robira, Bot. Rev. 35 (1969) 35.
[15] E.A. Paul, F.E. Clark, Soil Microbiology and Biochemistry, Academic Press, San Diego, CA, 1989.
[16] A. Leonard, G.B. Gerber, C. Stecca, J. Rueff, H. Borba, P.B. Farmer, R.J. Sram, A.E. Czeizel, I. Kalina, Mut. Res. 436 (1999) 263.
[17] J.M. Wyatt, C.J. Knowles, Biodegradation 6 (1995) 93.
[18] R.A. Woutersen, Scand. J. Work. Environ. Health 24 (1998) 5.
[19] E. Delzell, R.R. Monson, J. Occup. Med. 24 (1982) 767.
[20] A.E. Czeizel, S.L. Timar-Hegedus, Mut. Res. 427 (1999) 105.
[21] H. Kidd, D.R. James, The Agrochemicals Handbook, 3rd ed., Royal Society of Chemical Information Services, Cambridge, UK, 1998.
[22] US National Library of Medicine, Hazardous Substances Databank, Bethesda, MD, 1995.
[23] J.M. Wyatt, E.A. Linton, Cyba Found. Symp. 140 (1988) 32.
[24] Y. Asano, K. Fujishiro, Y. Tani, H. Yamada, Agric. Biol. Chem. 46 (1982) 1165.
[25] T. Amarant, Y. Vered, Z. Bohak, Biotechnol. Appl. Biochem. 11 (1989) 49.
[26] Y. Tani, M. Kurihara, H. Nishise, Agric. Biol. Chem. 53 (1989) 3151.
[27] T. Nagasawa, K. Ryuno, H. Yamada, Biochem. Biophys. Res. Commun. 139 (1986) 1305.
[28] J.L. Moreau, S. Azza, A. Arnaud, P. Galzy, J. Basic Microbiol. 33 (1993) 323.
[29] T. Nagasawa, H. Nanba, K. Ryuno, K. Takeuchi, H. Yamada, Eur. J. Biochem. 162 (1987) 691.
[30] M. Kobayashi, M. Nishiyama, T. Nagasawa, S. Horinouchi, T. Beppu, H Yamada, Biochim. Biophys. Acta 1129 (1991) 23.
[31] T. Nagamune, J. Honda, W.D. Cho, N. Kamiya, Y. Teratani, A. Hirata, H. Sasabe, I. Endo, J. Mol. Biol. 220 (1991) 221.
[32] M.R. Kaakeh, J.L. Legras, R. Duran, A. Chion-Arnaud, P. Galzy, Zentbl. Mikrobiol. 146 (1991) 89.
[33] W.Z. Li, Y.Q. Zhang, H.F. Yangm, Appl. Biochem. Biotechnol. 36 (1992) 171.
[34] T. Nagasawa, K. Takeuchi, H. Yamada, Eur. J. Biochem. 196 (1991) 581.
[35] M.S. Payne, S. Wu, R.D. Fallon, G. Tudor, B. Stieglitz, I.M. Turner, M.J. Nelson, Biochemistry 36 (1997) 5447.
[36] S. Wu, R.D. Fallon, M.S. Payne, Appl. Microbiol. Biotechnol. 48 (1997) 704.
[37] T. Nagasawa, K. Ryuno, H. Yamada, Experientia 45 (1989) 1066.

[38] T. Nagasawa, H. Shimizu, H. Yamada, Appl. Microbiol. Biotechnol. 40 (1993) 189.
[39] R. Padmakumar, P. Oriel, Appl. Biochem. Biotechnol. 77 (1999) 671.
[40] K. Matoishi, A. Sana, N Imai, T. Yamazaki, M. Yokoyama, T. Sugai, H. Ohta, Tetrahedron: Asymmetry 9 (1998) 1097.
[41] T. Sugai, T. Yamazaki, M. Yokoyama, H. Ohta, Biosci. Biotechnol. Biochem. 61 (1997) 1419.
[42] A. Stolz, S. Trott, M. Binder, R. Bauer, B. Hirrlinger, N. Layh, H.-J. Knackmuss, J. Mol. Catal. B—Enzymatic 5 (1998) 137.
[43] R. Bauer, H.-J. Knackmuss, A. Stolz, Appl. Microbiol. Biotechnol. 49 (1998) 89.
[44] S.J. Maddrell, N.J. Turner, A. Kerridge, A.J. Willetts, J. Crosby, Tetrahedron Lett. 37 (1996) 6001.
[45] H. Kakeya, N. Sakai, T. Sugai, H. Ohta, Tetrahedron Lett. 32 (1991) 1343.
[46] M. Kobayashi, S. Shimizu, Nat. Biotechnol. 16 (1998) 733.
[47] L.Y. Young, C.E. Cerniglia, Microbial Transformation and Degradation of Toxic Organic Chemicals, Wiley–Liss Inc, New York, 1995.
[48] J.M. Wyatt, K.C. Knowles, Int. Biodeterior. Biodegrad. 35 (1995) 227.
[49] G.R.V. Babu, C.S. Chetty, J.H. Wolfram, K.D. Chapatwala, J. Environ. Sci. Health Part A—Environ. Sci. Eng. 29 (1994) 1957.
[50] Y. Sugiura, J. Kuwahara, T. Nagasawa, H. Yamada, J. Am. Chem. Soc. 109 (1987) 5848.
[51] L. Que Jr., R.Y.N. Ho, Chem. Rev. 96 (1996) 2607.
[52] A.L. Feig, S.J. Lippard, Chem. Rev. 94 (1994) 759.
[53] T. Noguchi, J. Honda, T. Nagamune, H. Sasabe, Y. Inoue, I. Endo, FEBS Lett. 358 (1995) 9.
[54] T. Noguchi, M. Hoshino, M. Tsujimura, M. Odaka, Y. Inoue, I. Endo, Biochemistry 35 (1996) 16777.
[55] M. Tsujimura, M. Odaka, S. Nagashima, M. Yohda, I. Endo, J. Biochem. 119 (1996) 407.
[56] M. Odaka, K. Fuji, M. Hoshino, T. Noguchi, M. Tsujimura, S. Nagashima, M. Yohda, T. Nagamune, Y. Inoue, I. Endo, J. Am. Chem. Soc. 119 (1997) 3785.
[57] W. Huang, J. Jia, J. Cummings, M. Nelson, G. Schneider, Y. Lindqvist, Structure 5 (1997) 691.
[58] S. Nagashima, M. Nakasako, N. Dohmae, M. Tsujimura, K. Takio, M. Odaka, M. Yohda, N. Kamiya, I. Endo, Nat. Struct. Biol. 5 (1998) 347.
[59] Endo and coworkers [58] pointed out that the electron densities of the oxygen atoms corresponding to the post-translationally modified cysteine residues did not appear until the resolution in the structure refinement was higher than 2.3 Å and this explains why Nelson and coworkers [57] could not identify such groups in their study at 2.65 Å resolution.
[60] M. Tsujimura, N. Dohmae, M. Odaka, M. Chijimatsu, K. Takio, M. Yohda, M. Hoshino, S. Nagashima, I. Endo, J. Biol. Chem. 272 (1997) 29454.
[61] J.W. Peters, M.H.B. Stowell, S.M. Soltis, M.G. Finnegan, M.K. Johnson, D.C. Rees, Biochemistry 36 (1997) 1181.
[62] T. Murakami, M. Nojiri, H. Nakayama, M. Odaka, M. Yohda, N. Dohmae, K. Takio, T. Nagamune, I. Endo, Protein Sci. 9 (2000) 1024.
[63] M.J. Nelson, H. Jin, I.M. Turner Jr., G. Grove, R.C. Scarrow, B.A. Brennan, L. Que Jr., J. Am. Chem. Soc. 113 (1991) 7072.
[64] P.E. Doan, M.J. Nelson, H. Jin, B.M. Hoffman, J. Am. Chem. Soc. 118 (1996) 7014.
[65] M. Kobayashi, S. Shimizu, Eur. J. Biochem. 261 (1999) 1.
[66] B.A. Brennan, G. Alms, M. Nelson, L.T. Durney, R.C. Scarrow, J. Am. Chem. Soc. 118 (1996) 9194.
[67] C.M. Jensen, W.C. Trogler, J. Am. Chem. Soc. 108 (1986) 723.
[68] R.A. Michelin, M. Mozzon, R. Bertani, Coord. Chem. Rev. 147 (1996) 299.
[69] J.A. Ibers, R.H. Holm, Science 5 (1980) 157.
[70] D.S. Marlin, P.K. Mascharak, Chem. Soc. Rev. 29 (2000) 69.
[71] R.H. Holm, J.A. Ibers, Iron–Sulfur Proteins, vol. III, Academic Press, New York, 1977 (chap. 7).
[72] E. Deutsch, M.J. Root, D.L. Nosco, Adv. Inorg. Bioinorg. Mech. 1 (1982) 269.
[73] K.J. Ellis, A.G. Lappin, A.J. McAuley, J. Chem. Soc. Dalton Trans. (1975) 1931.
[74] M. Sigel, R.B. Martin, Chem. Rev. 82 (1982) 385.
[75] S.J. Lippard, Angew. Chem. Int. Ed. Engl. 27 (1988) 344.
[76] G.D. Fallon, B.M. Gatehouse, J. Chem. Soc. Dalton Trans. (1975) 1344.
[77] P.J. Marini, K.S. Murray, B.O. West, J. Chem. Soc. Dalton Trans. (1983) 143.
[78] S.C. Shoner, D. Barnhart, J.A. Kovacs, Inorg. Chem. 34 (1995) 4517.
[79] A.L. Nivorozhkin, A.I. Uraev, G.I. Bondarenko, A.S. Antsyshkina, V.P. Kurbatov, A.D. Garnovskii, C.I. Turta, N.D. Brashoveanu, Chem. Commun. (1997) 1711.
[80] L.F. Lindoy, S.E. Livingstone, Inorg. Chim. Acta 1 (1967) 365.
[81] J.C. Noveron, R. Herradora, M.M. Olmstead, P.K. Mascharak, Inorg. Chim. Acta 285 (1999) 269.
[82] J.-P. Costes, F. Dahan, J.-P. Laurent, Inorg. Chem. 29 (1990) 2448.
[83] K. Ramesh, R. Mukherjee, J. Chem. Soc. Dalton Trans. (1992) 83.
[84] M. Tweedle, L.J. Wilson, J. Am. Chem. Soc. 98 (1976) 4824.
[85] C. Butzlaff, A.X. Trautwein, T. Beissel, K.S. Burger, V. Gottfried, K. Wieghardt, Inorg. Chem. 32 (1993) 124.
[86] J.J. Ellison, A. Nienstedt, S.C. Shoner, D. Barnhart, J.A. Cowen, J.A. Kovacs, J. Am. Chem. Soc. 120 (1998) 5691.
[87] D. Schweitzer, J.J. Ellison, S.C. Shoner, S. Lovell, J.A. Kovacs, J. Am. Chem. Soc. 120 (1998) 10996.
[88] R.C. Scarrow, B.S. Strickler, J.J. Ellison, S.C. Shoner, J.A. Kovacs, J.G. Cummings, M.J. Nelson, J. Am. Chem. Soc. 120 (1998) 9237.
[89] J.C. Noveron, M.M. Olmstead, P.K. Mascharak, Inorg. Chem. 37 (1998) 1138.
[90] S.J. Brown, M.M. Olmstead, P.K. Mascharak, Inorg. Chem. 29 (1990) 3229.
[91] X. Tao, D.W. Stephan, P.K. Mascharak, Inorg. Chem. 26 (1987) 754.
[92] M. Ray, D. Ghosh, Z. Shirin, R. Mukherjee, Inorg. Chem. 36 (1997) 3568.
[93] D.S. Marlin, M.M. Olmstead, P.K. Mascharak, Inorg. Chim. Acta 297 (2000) 106.
[94] D.S. Marlin, M.M. Olmstead, P.K. Mascharak, Inorg. Chem. 38 (1999) 3258.
[95] L.A. Tyler, J.C. Noveron, M.M. Olmstead, P.K. Mascharak, Inorg. Chem. 38 (1999) 616.
[96] J.C. Noveron, M.M. Olmstead, P.K. Mascharak, J. Am. Chem. Soc. 123 (2001) 3247.
[97] I. Artaud, S. Chatel, A.S. Chauvin, D. Bonnet, M.A. Kopf, P. Leduc, Coord. Chem. Rev. 190–192 (1999) 577.
[98] J. Hans, H.J. Krüger, Angew. Chem. 35 (1996) 2827.
[99] L. Heinrich, Y. Li, J. Vaissermann, G. Chottard, J.C. Chottard, Angew. Chem. Int. Ed. Engl. 38 (1999) 3526.
[100] L.A. Tyler, J.C. Noveron, M.M. Olmstead, P.K. Mascharak, Inorg. Chem. 39 (2000) 357.
[101] J.C. Noveron, M.M. Olmstead, P.K. Mascharak, J. Am. Chem. Soc. 121 (1999) 3553.
[102] F.A. Chavez, C.V. Nguyen, M.M. Olmstead, P.K. Mascharak, Inorg. Chem. 35 (1996) 6282.
[103] S. Chatel, M. Rat, S. Dijols, P. Leduc, J.P. Tuchagues, D. Mansuy, I. Artaud, J. Inorg. Biochem. 80 (2000) 239.
[104] I. Kung, D. Schweitzer, J. Shearer, W.D. Taylor, H.L. Jackson, S. Lovell, J.A. Kovacs, J. Am. Chem. Soc. 122 (2000) 8299.
[105] J. Shearer, I.Y. Kung, S. Lovell, W. Kaminsky, J.A. Kovacs, J. Am. Chem. Soc. 123 (2001) 463.